Published in final edited form as:
Heart Rhythm. 2014 October ; 11(10): 1693–1700. doi:10.1016/j.hrthm.2014.05.018.

Image-Based Left-Ventricular Shape Analysis for Sudden Cardiac Death Risk Stratification

Fijoy Vadakkumpadan, PhD[1], **Natalia Trayanova, PhD, FHRS**[1], and **Katherine C. Wu, MD**[2]

[1]Department of Biomedical Engineering and Institute for Computational Medicine, Johns Hopkins University, Baltimore, MD 21218, USA

[2]Division of Cardiology, Department of Medicine, Johns Hopkins Medical Institutions, Baltimore, MD 21287, USA

Abstract

Background—Low left-ventricular ejection fraction (LVEF), the main criterion used in current clinical practice to stratify sudden cardiac death (SCD) risk, has very low sensitivity and specificity.

Objective—To uncover indices of LV shape that differ between patients with a high risk of SCD and those with a low risk.

Methods—Utilizing clinical cardiac magnetic resonance (CMR) imaging and computational anatomy tools, a novel computational framework to compare three-dimensional (3D) LV endocardial surface curvedness, wall thickness (WT), and relative wall thickness (RWT) between patient groups was implemented. The framework was applied to CMR data of 61 patients with ischemic cardiomyopathy who were selected for prophylactic implantable cardioverter defibrillator treatment based on reduced LVEF. The patients were classified by outcome: group 0 had no events; group 1, arrhythmic events, and group 2, heart failure (HF). Segmental differences in LV shape were assessed.

Results—Global LV volumes and mass were similar amongst groups. Compared to patients with no events, patients in groups 1 and 2 had lower mean shape metrics in all coronary artery regions, with statistical significance in 9 comparisons, reflecting wall thinning and stretching/flattening.

Conclusions—Among patients with ischemic cardiomyopathy and low LVEF, there exist quantifiable differences in 3D endocardial surface curvedness, LVWT, and LVRWT between those with no clinical events, and those with arrhythmic or HF outcomes, reflecting adverse LV remodeling. This retrospective study is a proof-of-concept to demonstrate that regional LV remodeling indices have the potential to improve personalized risk assessment for SCD.

Corresponding author: Fijoy Vadakkumpadan, Department of Biomedical Engineering, and, Institute for Computational Medicine, Johns Hopkins University, 3400 N Charles St, Hackerman 217B, Baltimore, MD 21218, USA, fijoy@jhu.edu, Ph: 410 516 3322.

Conflicts of interest: None

Keywords

Sudden cardiac death; Cardiac magnetic resonance imaging; Computational anatomy; Shape analysis; Risk stratification; Implantable cardioverter defibrillator

INTRODUCTION

Sudden cardiac death (SCD) is a major health problem worldwide, affecting hundreds of thousands of persons annually in the United States alone.[1] As only a small fraction of victims survive an episode of SCD, it is of paramount importance to identify patients at risk, and give them prophylactic treatment. It is also crucial that the patient identification method is very specific, as implantable cardioverter defibrillator (ICD) therapy, the most widespread preventive care for SCD, is costly and associated with serious risks.[1] However, the patient selection criterion used in the current clinical practice, namely left ventricular ejection fraction (LVEF) ≤ 35%, has very low sensitivity and specificity.[2] Though numerous alternatives to SCD risk stratification have been proposed, the optimal approach remains unknown.[3]

It has been known for decades that cardiomyopathies are associated with adverse remodeling of LV geometry, including LV dilation, wall thinning, and shape alterations, and that this remodeling predicts overall morbidity and cardiovascular mortality.[4] Patient-specific LV geometry can now be analyzed with unprecedented accuracy, with recent advances in image-based data acquisition and analysis. On one hand, clinical cardiac magnetic resonance (CMR) imaging and its combination with late gadolinium enhancement (LGE) can effectively and non-invasively acquire global indices of three dimensional (3D) LV structure in health and disease.[1] On the other, the new field of computational anatomy offers rigorous mathematical and algorithmic tools for the detailed assessment of segmental differences in image-based cardiac geometry.[5] Leveraging these advances to incorporate regional metrics of LV remodeling may help identify patients at higher versus lower risk of SCD. Ideally, an anatomic biomarker could also differentiate patients with high risk of SCD from those who do not have SCD outcomes but instead eventually succumb to heart failure (HF), which is an important competing cause of death in cardiomyopathy patients, and for which the management approach can be quite different.

The overarching goal of our research is to uncover novel, image-based, 3D indices of LV geometry that can be utilized to predict SCD risk specifically. The present study is a proof-of-concept, in which we have implemented a framework that utilizes CMR, advanced image processing, and computational anatomy tools, to compare 3D LV endocardial surface curvature, wall thickness (WT), and relative wall thickness (RWT) between patient groups. We have retrospectively applied our methodology to data from ischemic cardiomyopathy patients who were selected for ICD implantation based on reduced LVEF, followed after implantation for clinical events, and divided into groups with differing SCD risk based on the follow-up. We hypothesized that 3D LV shape metrics could identify patients at highest risk for SCD. We also explored whether shape metrics alone could differentiate between SCD and HF outcomes.

METHODS

Our framework is outlined in Fig. 1, which shows how a patient heart image is processed with our pipeline, including reconstruction of 3D LV geometry, segmentation of endocardial surface, computation of 3D shape metrics, and region-wise statistical analysis. The data acquisition and the components of the pipeline are described in the following.

Data acquisition

Data used for the present study consisted of LGE-CMR images of 61 patients with ischemic cardiomyopathy and LVEF ≤ 35%, which represented a random sample from the CMR arm of the prospective observational study of implantable cardioverter defibrillators (CMR-PROSE-ICD) at Johns Hopkins University. [1] In CMR-PROSE-ICD, all patients were imaged, implanted with ICDs for primary prevention of SCD, and then followed for events, including appropriate ICD firings, sudden arrhythmic death (SAD), and death or hospitalization due to HF. We divided the 61 patients into three groups: group 0 consisted of 28 patients with no events during follow up, group 1 included 18 patients who either suffered from SAD or whose ICDs fired appropriately, and group 2 comprised of 15 patients who died of or were hospitalized for HF, but did not have an arrhythmic event. Patients who had both an arrhythmic event and HF were included in group 1. See Online Supplement, Section 1 for more details.

Reconstruction of 3D LV geometry

In each short-axis slice of the image, LV endocardium and epicardium were semi-automatically contoured. Septal part of the endocardial contour was then manually identified by placing two landmark points near the right-ventricular (RV) insertion points (Fig. 2A). Investigators who performed the contouring and landmark placement were blinded to the patient groups. From the contours and landmark points, three sets of 2D binary masks, each set implicitly representing the LV endocardium, LV epicardium, and septal endocardium were constructed (Fig. 2B). Each set of 2D masks was then interpolated to build a 3D binary mask at 1mm isotropic resolution.[6] Finally, the geometry image of the LV wall was generated by combining the three 3D masks (Fig. 2C). For more details, please see Online Supplement, Section 2.

Computation of shape metrics

For each image voxel along the endocardial surface, curvedness of the surface, as well as WT and RWT of the LV were computed. Curvedness characterizes the deviation of a surface from flatness, and is defined as the root mean square of principal curvatures.[7] We computed the principal curvatures as described in Goldman,[8] from a Gaussian-smoothed version of the 3D mask for the LV chamber illustrated in Fig. 2C. The WT at an endocardial surface voxel was calculated as the distance to the nearest voxel that lied along the epicardium. The RWT at an endocardial surface voxel was computed as the product of curvedness and WT at that voxel (Fig. 3). This definition of RWT is our 3D extension of a 2D echocardiographic concept,[9] where RWT is defined as the ratio of posterior or septal wall thickness to radius of the LV endocardium in diastole. Since curvedness is the inverse

of radius,[7] the product of curvedness and WT is a measure of RWT. For more details, please see the Online Supplement, Section 3.

Segmentation of patient endocardial surface

To perform localized statistical analysis, the endocardial surface of each patient LV geometry was segmented based on American Heart Association (AHA) myocardial regions[10] as well as local transmurality of the infarct. For details on the segmentation, please see Online Supplement, Section 4. Briefly, to automate the segmentation into AHA regions, one LV geometry (referred to as the atlas) was selected, and semi-automatically segmented into the AHA regions.[11] This atlas was then deformed to match each of the remaining patient LV geometries using affine transformation and the computational anatomy algorithm termed multi-channel large deformation diffeomorphic metric mapping (MC-LDDMM).[12] These deformations provided, for each point in the atlas, the anatomically corresponding points on patient LV geometries. Finally, each voxel on the endocardial surface of a patient LV geometry was classified as belonging to the same AHA region as the anatomically corresponding point on the atlas (Fig. 4A–D).

To segment the endocardial surface of a patient LV into transmurally infarcted regions and the rest, first the infarct zone was planimetered on each short-axis 2D slice.[1] Second, a 3D reconstruction of the infarct geometry was obtained at 1mm isotropic resolution, via a shape-based binary interpolation method.[13] Third, at each endocardial surface voxel v, a line segment was computed by connecting v to the nearest epicardial surface voxel, and the transmural extent of the infarct (TEI) at v was calculated as the proportion of this line segment that intersects with the 3D reconstruction of the infarct geometry. Finally, each endocardial surface voxel with TEI $\geq$ 75% was classified as transmurally infarcted (Fig. 4E–G). This particular threshold is often used to delineate transmural scar.[14]

Statistical analyses

Baseline characteristics were summarized as means or proportions for each patient group, and statistically compared between groups. The 3D distribution of TEI was derived by calculating, at each point on the atlas endocardial surface, the mean and standard deviation (SD) of TEIs at points on patient LVs that corresponded to p according to the deformations of the atlas geometry. Similarly, the distributions of the shape metrics were also generated. Mean TEI in each of the three coronary arterial territories, namely left anterior descending artery (LAD), right coronary artery (RCA), and left circumflex artery (LCX), were calculated based on segmentation of the atlas endocardium into AHA regions, and the correspondence between the AHA regions and the territories.[10] AHA region 17 was excluded from all analyses because of limited image resolution at the apex (see Online Supplement, Section 1). Differences in the mean TEI between groups, and between coronary artery territories were examined. In each of the coronary artery regions of each patient, mean of each shape metric was calculated as the average of the metric at all points in the region, and differences in mean of the shape metrics between pairs of groups were assessed. For each patient group, and for each coronary artery region, differences in mean of the shape metrics between transmurally infarcted areas and the rest were evaluated. In all statistical comparisons, correction for covariates was performed using linear regression, and multiple

comparison errors were eliminated with permutation tests. For more details, refer to Online Supplement, Section 5.

RESULTS

Baseline characteristics

Baseline characteristics of the patient cohort are summarized in Table I. The mean follow up time for patients without events was 8.4±0.7 years. All characteristics were statistically insignificant, but diabetes ($P = 0.06$) was more prevalent in group 2 and CMR LVEF ($P = 0.17$) trended lower in group 1. Fig. 5 shows the anterior view of the spatial distribution of TEI in the patient cohort, as well as comparisons of the mean TEI between groups, and between coronary artery territories. The mean TEI in the LAD region was significantly higher in 4 comparisons. There was only one significant inter-group comparison, but in general, TEI did not differ between outcome groups. Fig. 5 also displays the spatial distributions of the shape metrics in the entire patient cohort.

Shape differences between outcome groups within coronary artery regions

Fig. 6 shows comparison of the shape metrics between groups in each of the coronary artery regions. In all regions, groups with an event had lower mean curvedness, WT, and RWT. Out of the 27 inter-group comparisons, 9 were statistically significant. Among the three shape metrics, the maximum number of significant differences was found in RWT. There were no significant differences in the shape metrics between groups 1 and 2.

Shape differences within outcome groups between transmurally infarcted and the remaining regions

Fig. 7 shows, within each patient outcome group, and within each coronary artery subdivision, comparisons of the shape metrics between transmurally infarcted regions, and either non-transmurally infarcted or normal regions. In all but four comparisons, and in all significant comparisons, the shape metrics were lower in transmurally infarcted areas. Four of the 8 significant comparisons involved the LAD coronary artery territory, reflecting increased LV remodeling in this territory due to transmural infarction.

DISCUSSION

This research aimed to investigate whether or not image-based 3D regional indices of LV geometry can differentially identify SCD risk. To this end, we implemented a proof-of-concept framework, which is novel in that it combines CMR and computational anatomy. We applied the methodology to a cohort of patients with ischemic cardiomyopathy and LV dysfunction, and revealed, for the first time, that differences in local 3D LV endocardial curvedness, WT, and RWT can be identified between those with no events during clinical follow up, and those with arrhythmic or HF events, despite similar global indices of remodeling (LV volumes and mass). Our results also suggest that the LV anatomical substrate may be similar in patients who are susceptible to either ventricular arrhythmias or HF. Hence, LV anatomical parameters alone may not be able to definitively differentiate between the two competing causes of death in cardiomyopathy patients, i.e. sudden

arrhythmic death and pump failure. Nonetheless, incorporating the proposed shape metrics into SCD risk prediction has the potential to help enhance the accuracy of image-based risk stratification approaches by accounting for individual differences in regional LV anatomy that are not adequately described by the currently used global LV metrics, and identifying a cohort with favorable LV anatomy that portends good prognosis.

Previous studies have shown that global LV volume and mass are associated with a composite of cardiovascular events post-infarction.[9] In addition, it is known that global LV shape, as measured in 2D approaches by the so-called sphericity index, can predict adverse clinical outcomes, including cardiovascular death and HF, even after controlling for LV volumes.[15, 16] Also, categorization of LV geometry into four classes based on LV mass index and RWT measured from 2D or M-mode echocardiograms has recently been found to be associated with cardiovascular risk.[9] Despite the numerous efforts to correlate indices of LV remodeling with clinical outcomes, it remains unknown whether these indices, especially those that characterize LV shape, can be useful in predicting SCD risk. Furthermore, the LV shape indices in existing studies are restricted to 2D global measurements. Qualitatively, since the same 2D global measurement can correspond to any number of 3D shapes, as in the example of the 2D sphericity index, the discriminability of 2D indices is poor.[17] In the present study, we have developed a state-of-the-art computational framework to statistically compare 3D indices of regional LV shape between patient groups, and utilized this framework to demonstrate differences between patients with a low risk of SCD, and those with a high risk. A further quantitative comparison of global 2D and regional 3D metrics is needed to conclusively demonstrate the superiority of the latter.

Our patient cohort was fairly typical of others with ischemic cardiomyopathy.[18] There was a predominance of scar involving the LAD distribution, with a lesser prevalence of scar in the RCA and LCX territories. The magnitude of LV curvedness and WT values in the current study are comparable to those published elsewhere for patients with ischemic cardiomyopathy.[7, 11] In addition, it is clear from Fig. 5 that, as one proceeds from the base to apical portions of the LV, the curvedness increases, and WT decreases, as expected.[19, 20] Incidentally, only computational anatomy techniques such as the ones we employ in this study can generate the 3D distributions in Fig. 5. Our results are consistent with previous studies which showed that global LV dilation and wall thinning post-infarction correlate with adverse cardiovascular events.[4] Further, our study provides novel findings in demonstrating that the differences in curvedness, WT, and RWT exist locally throughout the LV, as well as between patients without events, and those with specifically arrhythmic or HF events. Notably, it remains unknown whether LV shape analysis can be used to differentiate arrhythmic and heart failure patients, as our study revealed no significant differences between these two groups. Similar LV shape changes can predispose patients to both ventricular arrhythmias and heart failure complications due to heterogeneity in LV mechanics, but for clinical management, one would ideally be able to differentiate the two. Our results suggest that LV shape metrics alone may be insufficient for this purpose, and future studies could combine other biomarkers with LV shape indices. Nonetheless, our findings remain important in that 3D shape analysis was able to differentiate patients without events from those with events. Hence, one may be able to improve identification of

the low risk population by the lack of significant regional LV remodeling in 3D shape analysis. Those patients who do have significant regional LV remodeling may benefit from more aggressive heart failure therapies as well as prophylactic ICDs. Our results in Fig. 7 demonstrate that the shape metrics were lower in transmurally infarcted areas, and the most pronounced differences occurred in the LAD territory. This corroborates existing evidence indicating that transmurally infarcted regions expand, and this occurs more commonly in the anterior, anteroseptal, and anteroapical regions.[21, 22]

Mechanistically, it has been postulated that LV dilation and wall thinning, similarly to those illustrated in Fig. 6, lead to worse arrhythmic outcomes because of increased wall strain and stress, which in turn trigger stretch-activated ion channels.[23, 24] Also, LV remodeling is correlated with infarct size,[25, 26] and so are arrhythmic events.[27] The increased wall stress caused by LV dilation and thinning also elicit compensatory responses, and when these responses are inadequate, a vicious cycle of further dilation ensues, and the heart eventually fails.[25, 28] Note that increases in wall stress are believed to be the principal change that occurs during LV remodeling,[4] and our RWT metric accounts for both radius of curvature and WT, the two geometric parameters that contribute to wall stress.[29] Hence, of the three shape metrics we considered in this study, RWT produced the maximum number of significant differences between patients with and without events.

The novel computational framework and findings in this study constitute an important step toward utilization of LV shape indices in clinical risk stratification of cardiomyopathy patients. We envision that the shape indices we propose could potentially be used in combination with existing predictors of SCD such as LV and scar volumes, to train a statistical model, which, given the shape metrics of a patient, may non-invasively and reliably compute a personalized risk score that reflects the patient's susceptibility to SCD. The framework that we have developed is equally applicable to patients with non-ischemic etiologies or with LVEF ≥ 35%, and can incorporate any point-wise shape metric. Similarly, our methodology can be straightforwardly extended to use other clinical imaging modalities such as cine MRI sequences or cardiac computed tomography.

A limitation of the present methodology is that the contouring of endo- and epicardial boundaries requires significant manual intervention, which is time consuming. Planimetry techniques that are more automated[30] may be incorporated into our framework. The lack of statistical significance in some inter-group comparisons is a drawback of our results. However, we show that groups with events have lower shape metrics in all comparisons, and it is expected that some of the non-significant comparisons will become significant as sample size is increased. Also, only end-diastolic images are used in this study. Our framework can be extended to utilize the end systolic phase, where the effects of LV remodeling are more pronounced,[7, 29] and to analyze change in shape metrics over the cardiac cycle.

CONCLUSIONS

We have developed a novel methodology that employs CMR and computational anatomy tools to detect regional differences in 3D LV shape between patient groups. Utilizing this

methodology, we showed that, among post-infarct, low LVEF patients, there exist differences in LV endocardial curvedness, WT, and RWT between those with no clinical events, and those who develop arrhythmic or heart failure events. This retrospective study is a proof-of-concept supporting additional research to investigate the use of LV shape metrics, likely in combination with other risk markers, to improve SCD risk stratification, and potentially guide treatment delivery.

Supplementary Material

Refer to Web version on PubMed Central for supplementary material.

Acknowledgments

Sources of financial support: National Institutes of Health grants R01HL103812 (to KCW), R01HL103428 (to NT), and DP1HL123271 (to NT), and American Heart Association grant 13SDG14510061 (to FV).

Abbreviations

SCD	sudden cardiac death
LV	left ventricular
ICD	implantable cardioverter defibrillator
LVEF	left ventricular ejection fraction
3D	three-dimensional
CMR	cardiac magnetic resonance
LGE	late gadolinium enhancement
PROSE-ICD	prospective observational study of implantable cardioverter defibrillators
HF	heart failure
SAD	sudden arrhythmic death
RV	right ventricular
2D	two-dimensional
AHA	American heart association
MC-LDDMM	multi-channel large deformation diffeomorphic metric mapping
TEI	transmural extent of infarct
LAD	left anterior descending artery
RCA	right coronary artery
LCX	left circumflex artery
SD	standard deviation
WT	wall thickness
RWT	relative wall thickness

References

1. Wu KC, Gerstenblith G, Guallar E, Marine JE, Dalal D, Cheng A, Marbán E, Lima JAC, Tomaselli GF, Weiss RG. Combined Cardiac MRI and C-Reactive Protein Levels Identify a Cohort at Low Risk for Defibrillator Firings and Death. Circulation: Cardiovascular Imaging. 2012; 5:178–186. [PubMed: 22267750]
2. Santangeli P, Russo AD, Casella M, Pelargonio G, Di-Biase L, Natale A. Left ventricular ejection fraction for the risk stratification of sudden cardiac death: friend or foe? Internal Medicine Journal. 2011; 41:55–60. [PubMed: 21265961]
3. Lopera G, Curtis A. Risk stratification for sudden cardiac death: current approaches and predictive value. Current Cardiology Reviews. 2009; 5:56–64. [PubMed: 20066150]
4. Mann DL, Bristow MR. Mechanisms and Models in Heart Failure: The Biomechanical Model and Beyond. Circulation. 2004; 111:2837–2849. [PubMed: 15927992]
5. Beg MF, Helm PA, McVeigh E, Miller MI, Winslow RL. Computational Cardiac Anatomy Using MRI. Magnetic Resonance in Medicine. 2004; 52:1167–1174. [PubMed: 15508155]
6. Turk, G.; O'Brien, J. Shape Transformation Using Variational Implicit Functions. Proc. SIGGRAPH; 1999; p. 335-342.
7. Zhong L, Su Y, Yeo S-Y, Tan R-S, Ghista DN, Kassab G. Left ventricular regional wall curvedness and wall stress in patients with ischemic dilated cardiomyopathy. American Journal of Physiology - Heart and Circulatory Physiology. 2009; 296:H573–H584. [PubMed: 19122166]
8. Goldman R. Curvature formulas for implicit curves and surfaces. Computer Aided Geometric Design. 2005; 22:632–658.
9. Konstam MA, Kramer DG, Patel AR, Maron MS, Udelson JE. Left ventricular remodeling in heart failure: current concepts in clinical significance and assessment. Journal of Americal College of Cardiology: Cardiovascular Imaging. 2011; 4:98–108.
10. Cerqueira MD, Weissman NJ, Dilsizian V, Jacobs AK, Kaul S, Laskey WK, Pennell DJ, Rumberger JA, Ryan T, Verani MS. Standardized myocardial segmentation and nomenclature for tomographic imaging of the heart: a statement for healthcare professionals from the Cardiac Imaging Committee of the Council on Clinical Cardiology of the American Heart Association. Circulation. 2002; 105:539–542. [PubMed: 11815441]
11. Su Y, Zhong L, Lima C-W, Ghistac D, Chua T, Tan R-S. A geometrical approach for evaluating left ventricular remodeling in myocardial infarct patients. Computer Methods and Programs in Biomedicine. 2012; 108:500–510. [PubMed: 21507502]
12. Ceritoglu C, Oishi K, Li X, Chou MC, Younes L, Albert M, Lyketsos C, Zijl PCv, Miller MI, Mori S. Multi-contrast large deformation diffeomorphic metric mapping for diffusion tensor imaging. Neuroimage. 2009; 47:618–627. [PubMed: 19398016]
13. Raya SP, Udupa JK. Shape-based interpolation of multidimensional objects. IEEE Transactions on Medical Imaging. 1990; 9:32–42. [PubMed: 18222748]
14. Boyé P, Abdel-Aty H, Zacharzowsky U, Bohl S, Schwenke C, Geest RJvd, Dietz R, Schirdewan A, Schulz-Menger J. Prediction of life-threatening arrhythmic events in patients with chronic myocardial infarction by contrast-enhanced CMR. Journal of Americal College of Cardiology: Cardiovascular Imaging. 2011; 4:871–879.
15. Sutton MSJ, Plappert T, Rahmouni H. Assessment of Left Ventricular Systolic Function by Echocardiography. Heart Failure Clinics. 2009; 5:177–190. [PubMed: 19249687]
16. Wong SP, French JK, Lydon AM, Manda SO, Gao W, Ashton NG, White HD. Relation of left ventricular sphericity to 10-year survival after acute myocardial infarction. American Journal of Cardiology. 2004; 94:1270–1275. [PubMed: 15541243]
17. Salgo I, Tsang W, Ackerman W, Ahmad H, Chandra S, Cardinale M, Lang R. Geometric assessment of regional left ventricular remodeling by three-dimensional echocardiographic shape analysis correlates with left ventricular function. Journal of the American Society of Echocardiography. 2012; 25:80–88. [PubMed: 22000777]
18. Rott D, Nowatzky J, Weiss AT, Chajek-Shaul T, Leibowitz D. ST deviation pattern and infarct related artery in acute myocardial infarction. Clinical Cardiology. 2009; 32:E29–E32. [PubMed: 19816991]

19. Maffessanti F, Lang R, Niel J, Steringer-Mascherbauer R, Caiani E, Nesser H, Mor-Avi V. Three-dimensional analysis of regional left ventricular endocardial curvature from cardiac magnetic resonance images. Magnetic Resonance Imaging. 2011; 29:516–524. [PubMed: 21216552]

20. Ho SY. Anatomy and myoarchitecture of the left ventricular wall in normal and in disease. European Journal of Echocardiography. 2009; 10:iii3–iii7. [PubMed: 19889656]

21. McKay R, Pfeffer M, Pasternak R, Markis J, Come P, Nakao S, Alderman J, Ferguson J, Safian R, Grossman W. Left ventricular remodeling after myocardial infarction: a corollary to infarct expansion. Circulation. 1986; 74:693–702. [PubMed: 3757183]

22. Weisman HF, Healy B. Myocardial infarct expansion, infarct extension, and reinfarction: pathophysiologic concepts. Progress in Cardiovascular Diseases. 1987; 30:73–110. [PubMed: 2888158]

23. Miura M, Wakayama Y, Endoh H, Nakano M, Sugai Y, Hirose M, Keurs HET, Shimokawa H. Spatial non-uniformity of excitation-contraction coupling can enhance arrhythmogenic-delayed afterdepolarizations in rat cardiac muscle. Cardiovascular research. 2008; 80:55–61. [PubMed: 18558629]

24. Søgaard P, Gøtzsche CO, Ravkilde J, Nørgaard A, Thygesen K. Ventricular arrhythmias in the acute and chronic phases after acute myocardial infarction. Effect of intervention with captopril. Circulation. 1994; 90:101–107. [PubMed: 8025983]

25. Gaudron P, Eilles C, Kugler I, Ertl G. Progressive left ventricular dysfunction and remodeling after myocardial infarction. Potential mechanisms and early predictors. Circulation. 1993; 87:755–763. [PubMed: 8443896]

26. Cohn JN, Ferrari R, Sharpe N. Cardiac remodeling—concepts and clinical implications: a consensus paper from an international forum on cardiac remodeling. Journal of Americal College of Cardiology. 2000; 35:569–582.

27. Schmidt A, Azevedo CF, Cheng A, Gupta SN, Bluemke DA, Foo TK, Gerstenblith G, Weiss RG, Marban E, Tomaselli GF, Lima JA, Wu KC. Infarct tissue heterogeneity by magnetic resonance imaging identifies enhanced cardiac arrhythmia susceptibility in patients with left ventricular dysfunction. Circulation. 2007; 115:2006–14. [PubMed: 17389270]

28. Vannan M, Taylor D. Ventricular remodelling after myocardial infarction. British Heart Journal. 1992; 68:257–259. [PubMed: 1389754]

29. Zhong L, Su Y, Gobeawan L, Sola S, Tan RS, Navia JL, Ghista DN, Chua T, Guccione J, Kassab GS. Impact of surgical ventricular restoration on ventricular shape, wall stress, and function in heart failure patients. American Journal of Physiology: Heart and Circulatory Physiology. 2011; 300:H1653–H1660. [PubMed: 21357513]

30. Petitjean C, Dacher JN. A review of segmentation methods in short axis cardiac MR images. Medical Image Analysis. 2011; 15:169–184. [PubMed: 21216179]

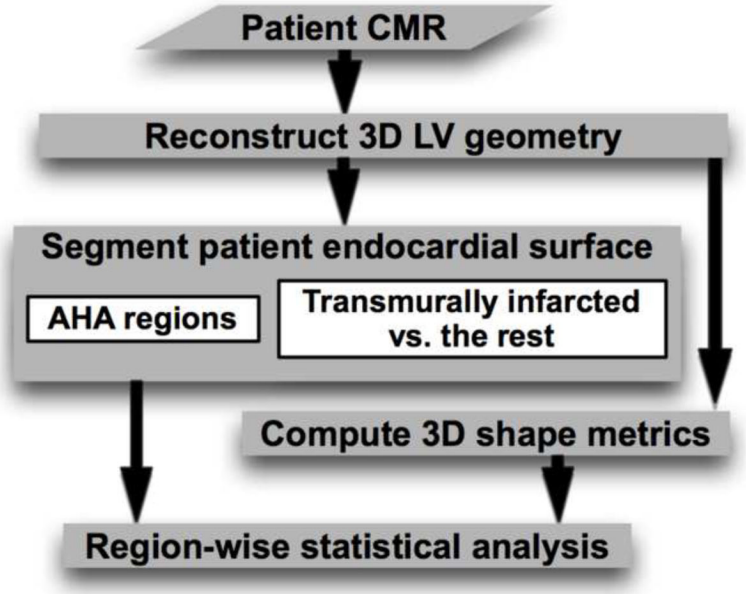

Figure 1.
The processing pipeline of our computational framework.

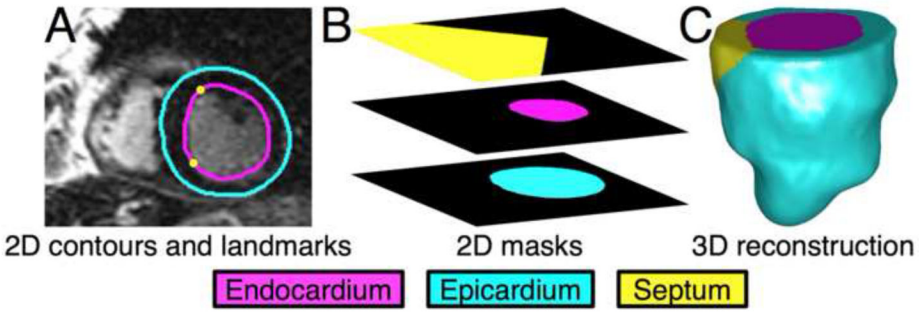

Figure 2.

Reconstruction of 3D LV geometry from CMR image slices. (A) Example slice with endocardial/epicardial contours, and landmarks corresponding to the septum. (B) The 2D endocardial, epicardial, and septal masks for the slice. (C) The reconstructed 3D geometry in anterior view.

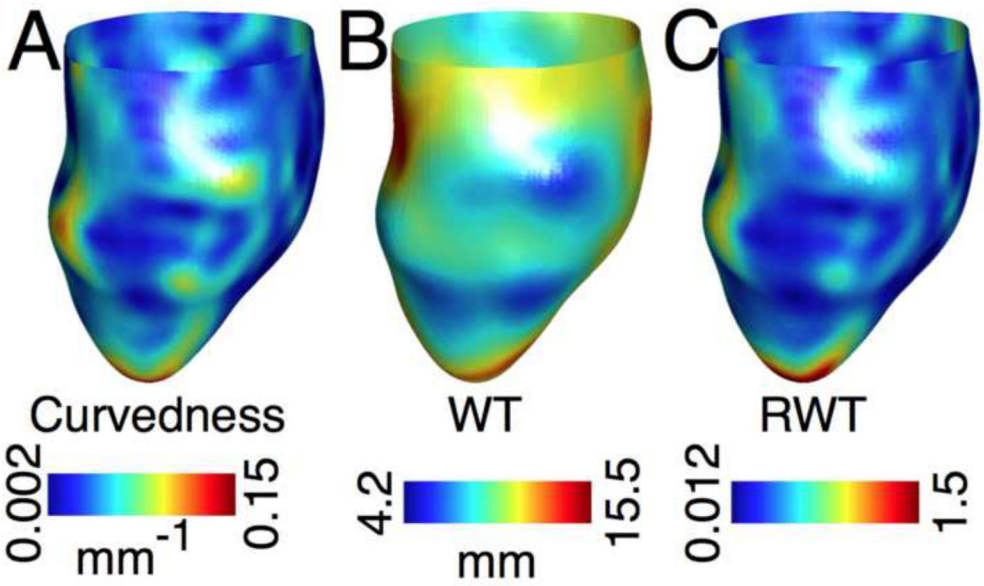

Figure 3.

Shape metrics computed for the LV geometry shown in Fig. 2C, displayed on the endocardial surface in anterior view. (A) Curvedness. (B) WT. (C) RWT.

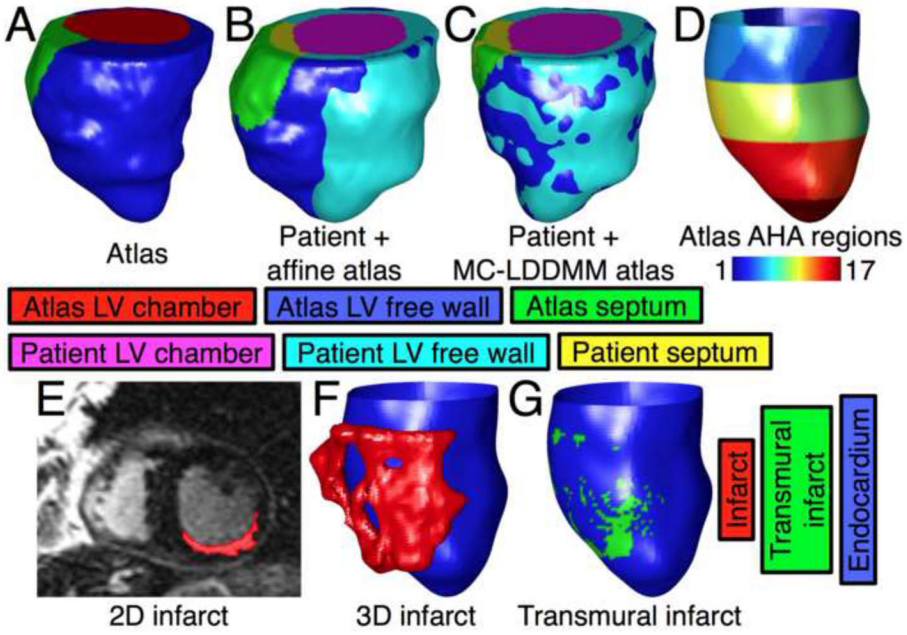

Figure 4.

Segmentation of endocardial surfaces of patients as described in the Methods section. (A) Atlas geometry in anterior view. (B) Superimposition of the patient heart geometry in Fig. 2C, and atlas geometry after affine transformation. (C) The patient heart geometry, and the atlas geometry after MC-LDDMM transformation. (D) Posterior view of segmentation of the endocardial surface of the patient heart geometry into the 17 AHA regions. (E) Segmentation of infarct region in an example 2D slice of the patient. (F) 3D reconstruction of the infarct region of the patient, along with the endocardial surface. (G) Segmentation of the endocardial surface of the patient into transmurally infarcted and the rest.

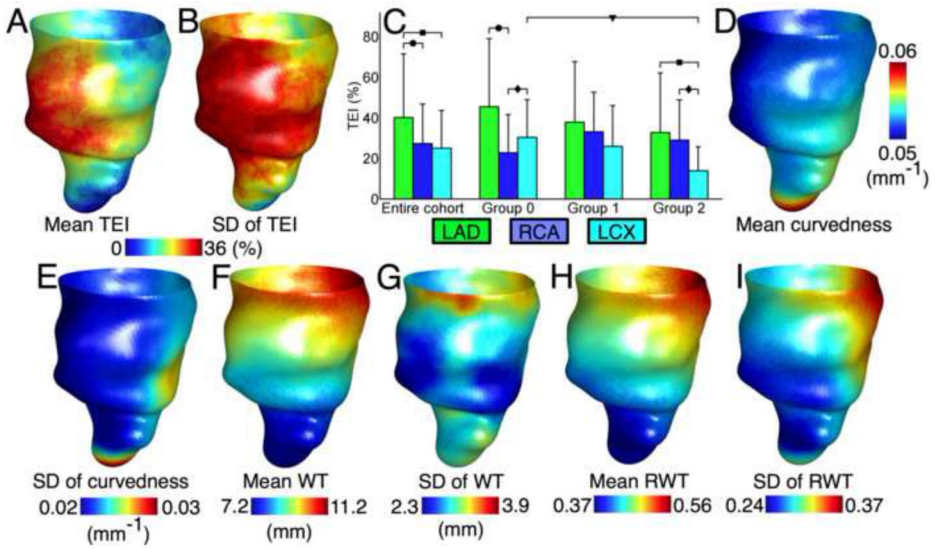

Figure 5.

Distributions of the TEI and the shape metrics. (A, and B) The mean and SD, respectively, of the TEI in the entire patient cohort, at each point on the 3D atlas endocardial surface in anterior view. (C) Mean and SD of transmural extent in the entire cohort and each of the patient groups, in each of the coronary artery territories. Brackets with different symbols indicate significant differences between patient groups for the same coronary artery region, and between coronary artery regions for the same group. (D, F, and H) The mean of curvedness, WT, and RWT, respectively, in the entire patient cohort at each point on the atlas endocardial surface in anterior view. (E, G, and I) The SD of curvedness, WT, and RWT, respectively, over the atlas endocardial surface.

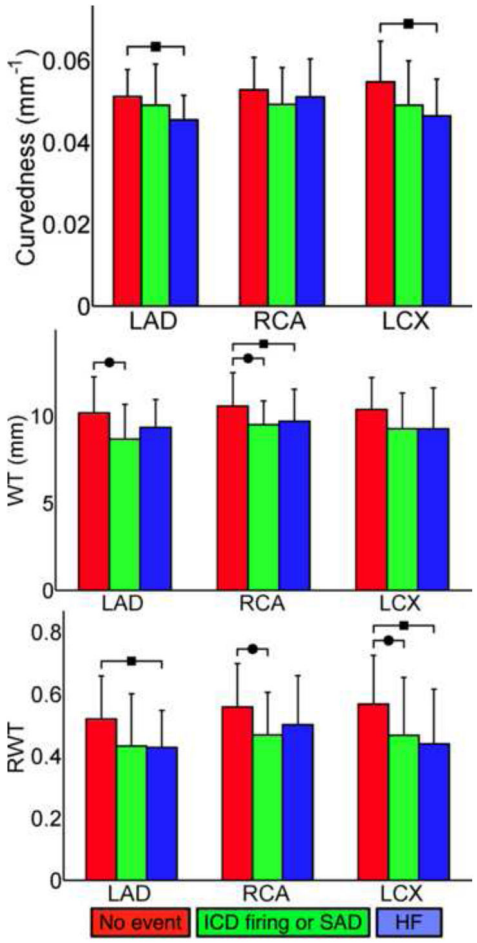

Figure 6.

Between group analysis: mean and SD of curvedness, WT, and RWT between each of the patient groups, and for each of the coronary artery regions. Brackets with different symbols indicate significant differences.

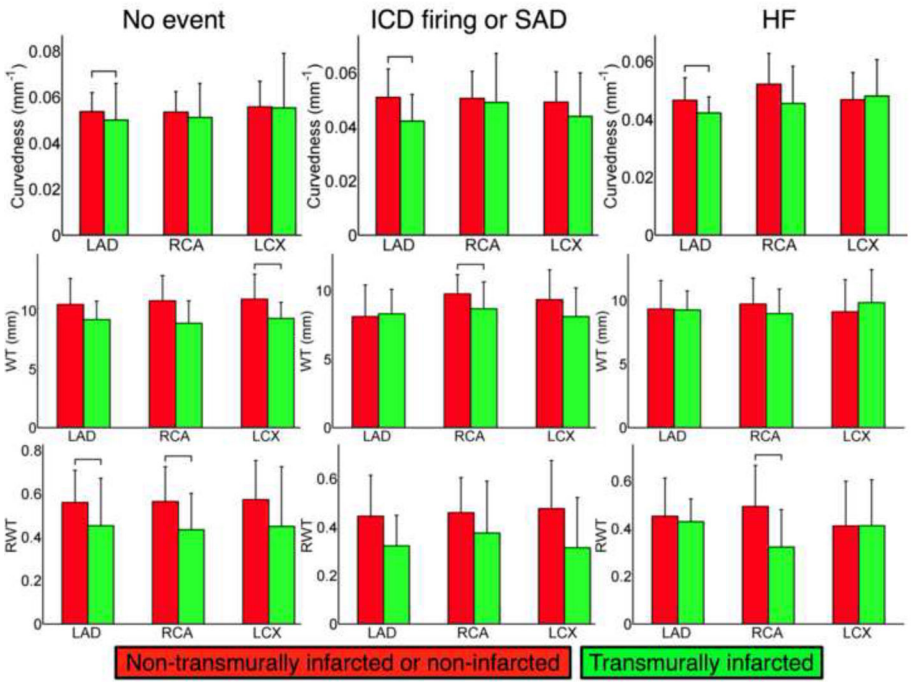

Figure 7.

Within group analysis: mean and SD of the shape metrics in the non-transmurally infarcted or normal, and transmurally infarcted regions, in each of the coronary artery, within each patient group (columns). Brackets indicate significant differences.

Table I

Baseline characteristics. Data are presented as mean ± SD or n (%).

	Group 0 (No event, n = 28)	Group 1 (ICD firing or SAD, n = 18)	Group 2 (HF, n = 15)	*P*
Male sex	23 (82)	14 (78)	12 (80)	0.97
Age	61.9 ± 10.7	61.0 ± 10.8	63.3 ± 11.1	0.89
Caucasian	23 (82)	16 (89)	12 (80)	0.89
Years from infarction incidence/diagnosis	8.1± 7.2	8.8 ± 6.0	5.9 ± 6.8	0.38
New York Heart Association function class				0.68
I	10 (36)	4 (22)	4 (27)	
II	9 (32)	9 (50)	4 (27)	
III	9 (32)	5 (28)	7 (46)	
Hypertension	23 (82)	11 (61)	11 (73)	0.49
Hypercholesterolemia	23 (82)	13 (72)	11 (73)	0.82
Diabetes	7 (25)	5 (28)	10 (67)	0.06
Nicotine use	20 (71)	15 (83)	10 (66)	0.68
Biventricular ICD	4 (14)	3 (17)	5 (33)	0.57
Enrollment LVEF (non-CMR), %	25.8 ± 6.7	22.1 ± 7.6	23.7 ± 6.8	0.27
CMR characteristics				
LVEF, %	30.0 ± 7.4	24.5 ± 9.0	29.2 ± 8.8	0.17
LV end-diastolic volume, mL	236.9 ± 67.0	238.1 ± 89.0	226.0 ± 63.4	0.90
LV end-systolic volume, mL	166.8 ± 55.3	181.8 ± 74.4	163.6 ± 62.4	0.74
LV mass, g	189.3 ± 53.4	168.1 ± 46.5	175.5 ± 55.0	0.41
Total infarct mass (LGE-CMR), g	36.6 ± 17.8	38.9 ± 18.7	38.8 ± 36.6	0.62

EF = ejection fraction; ICD = implantable cardioverter defibrillator; LGE-CMR = late gadolinium enhanced cardiac magnetic resonance imaging; LV = left ventricular; SAD = sudden arrhythmic death; HF = heart failure